Vol. 130: 11–24, 2018
https://doi.org/10.3354/dao03250

DISEASES OF AQUATIC ORGANISMS
Dis Aquat Org

Published August 28

Phylogenomic characterization of two novel members of the genus *Megalocytivirus* from archived ornamental fish samples

Samantha A. Koda[1], Kuttichantran Subramaniam[1], Ruth Francis-Floyd[2], Roy P. Yanong[3], Salvatore Frasca Jr.[4,8], Joseph M. Groff[5], Vsevolod L. Popov[6], William A. Fraser[7], Annie Yan[7], Shipra Mohan[7], Thomas B. Waltzek[1,*]

[1]Department of Infectious Diseases and Immunology, College of Veterinary Medicine, University of Florida, Gainesville, Florida 32611, USA

[2]Department of Large Animal Clinical Sciences, College of Veterinary Medicine, University of Florida, Gainesville, Florida 32608, USA

[3]University of Florida School of Forest Resources and Conservation, Program in Fisheries and Aquatic Sciences Tropical Aquaculture Laboratory, Ruskin, Florida 33570, USA

[4]Conneticut Veterinary Medical Diagnostic Laboratory, Department of Pathobiology and Veterinary Science, University of Connecticut, Storrs, Connecticut 06269, USA

[5]Fish Health Laboratory, School of Veterinary Medicine, University of California, Davis, California 95616, USA

[6]Department of Pathology, University of Texas Medical Branch, Galveston, Texas 77555, USA

[7]Florida Department of Agriculture and Consumer Services, Bronson Animal Disease Diagnostic Laboratory, Kissimmee, Florida 34741, USA

[8]*Present address:* Department of Comparative, Diagnostic, and Population Medicine, College of Veterinary Medicine, University of Florida, Gainesville, Florida 32610, USA

ABSTRACT: The genus *Megalocytivirus* is the most recently described member of the family *Iridoviridae*; as such, little is known about the genetic diversity of this genus of globally emerging viral fish pathogens. We sequenced the genomes of 2 megalocytiviruses (MCVs) isolated from epizootics involving South American cichlids (oscar *Astronotus ocellatus* and keyhole cichlid *Cleithracara maronii*) and three spot gourami *Trichopodus trichopterus* sourced through the ornamental fish trade during the early 1990s. Phylogenomic analyses revealed the South American cichlid iridovirus (SACIV) and three spot gourami iridovirus (TSGIV) possess 116 open reading frames each, and form a novel clade within the turbot reddish body iridovirus genotype (TRBIV Clade 2). Both genomes displayed a unique truncated paralog of the major capsid protein gene located immediately upstream of the full-length parent gene. Histopathological examination of archived oscar tissue sections that were PCR-positive for SACIV revealed numerous cytomegalic cells characterized by basophilic intracytoplasmic inclusions within various organs, particularly the anterior kidney, spleen, intestinal lamina propria and submucosa. TSGIV-infected grunt fin (GF) cells grown *in vitro* displayed cytopathic effects (e.g. cytomegaly, rounding, and refractility) as early as 96 h post-infection. Ultrastructural examination of infected GF cells revealed unenveloped viral particles possessing hexagonal nucleocapsids (120 to 144 nm in diameter) and electron-dense cores within the cytoplasm, consistent with the ultrastructural morphology of a MCV. Sequencing of SACIV and TSGIV provides the first complete TRBIV Clade 2 genome sequences and expands the known host and geographic range of the TRBIV genotype to include freshwater ornamental fishes traded in North America.

KEY WORDS: *Iridoviridae* · *Megalocytivirus* · *Infectious spleen and kidney necrosis virus* · Red seabream iridovirus · Turbot reddish body iridovirus · Phylogenomics · Genome · Keyhole cichlid · Oscar · Three spot gourami

*Corresponding author: tbwaltzek@ufl.edu

INTRODUCTION

The family *Iridoviridae* is composed of 5 genera of large double-stranded DNA viruses that infect arthropods (subfamily *Betairidovirinae*; genera *Chloriridovirus* and *Iridovirus*) or ectothermic vertebrates (subfamily *Alphairidovirinae*; genera *Lymphocystivirus*, *Ranavirus*, and *Megalocytivirus*). Megalocytiviruses (MCVs) display stereotypical iridovirus virion architecture including an electron-dense nucleocapsid with icosahedral symmetry ranging in size from 140 to 200 nm in diameter (Chinchar et al. 2017). *Infectious spleen and kidney necrosis virus* (ISKNV), originally reported from mandarin fish *Siniperca chuatsi* cultured in China (He et al. 2000, 2001), represents the type species in the monotypic genus *Megalocytivirus* (Chinchar et al. 2017). Closely related ISKNV strains have been characterized from a diverse range of finfish species (Kurita et al. 2002, Chen et al. 2003, Do et al. 2004, Lü et al. 2005, Shi et al. 2010, Zhang et al. 2013, Wen & Hong 2016, Shiu et al. 2018).

Phylogenetic analyses based on the major capsid protein and ATPase genes have revealed 3 ISKNV genotypes: a red seabream iridovirus (RSIV) genotype that includes strains from marine fishes in Japan, Korea, China, and Southeast (SE) Asia; an ISKNV genotype that includes strains from Chinese mandarin fish and ornamental fishes cultivated in SE Asia; and a turbot reddish body iridovirus (TRBIV) genotype that includes strains from Asian flatfishes (Do et al. 2005a, Shi et al. 2010, Go et al. 2016). Each of the MCV genotypes have been subdivided into 2 separate clades. The second clade of the TRBIV genotype was recently characterized from material derived from (1) MCV outbreaks in freshwater ornamental fishes from the late 1980s through the early 1990s (Go et al. 2016) and (2) a 2008 MCV outbreak involving rock bream *Oplegnathus fasciatus* fingerlings recently imported into Taiwan from Korea (Huang et al. 2011). The characterization of iridoviruses distantly related to ISKNV from threespine stickleback *Gasterosteus aculeatus* (Waltzek et al. 2012) and barramundi *Lates calcarifer* (de Groof et al. 2015) have led to the proposal of additional species in the genus *Megalocytivirus* (Chinchar et al. 2017). The high sequence identity exhibited by ISKNV genotypes as well as the discovery of unclassified iridoviruses distantly related to ISKNV (Waltzek et al. 2012, de Groof et al. 2015) has stimulated the International Committee on Taxonomy of Viruses study group on iridoviruses to begin re-evaluating the criteria (e.g. host range, gene order, the presence or absence of specific genes, genetic identity/similarity, antigenicity) to be used in defining MCV species (Chinchar et al. 2017).

Similar to some lymphocystiviruses and ranaviruses, MCVs lack host specificity and infect a range of tropical fishes from both freshwater and marine environments (Waltzek et al. 2012, Chinchar et al. 2017, Kawato et al. 2017). Since the first suspected case of MCV infection in ram cichlids *Mikrogeophagus ramirezi* (Leibovitz & Riis 1980), MCVs have been detected in more than 125 fish species across 11 orders and 44 families (Jung & Oh 2000, Kurita et al. 2002, Sudthongkong et al. 2002b, Gibson-Kueh et al. 2003, Jeong et al. 2003, Nakajima & Kurita 2005, Y. Q. Wang et al. 2007, Song et al. 2008, C. S. Wang et al. 2009, Yanong & Waltzek 2016, S. A. Koda & T. B. Waltzek unpubl. data). They induce lethal systemic diseases negatively impacting food fish and ornamental aquaculture industries (Sudthongkong et al. 2002a, Gibson-Kueh et al. 2003, Jeong et al. 2008b, Zhang et al. 2013, Go et al. 2016, Kawato et al. 2017). Waltzek et al. (2012) characterized an iridovirus related to MCVs in Canadian wild-caught threespine stickleback. RSIV has long been recognized as an important threat to Asian mariculture and is listed by the World Organization for Animal Health as a notifiable disease (OIE 2016b). The use of a formalin-inactivated vaccine has reduced the impact of RSIV disease on Japanese mariculture; however, its economic viability and effectiveness within ornamental aquaculture has not been established (Nakajima et al. 1997, 1999, Kawato et al. 2017).

Epizootiological evidence and experimental studies suggest MCVs are transmitted horizontally through cohabitation (He et al. 2002, Go & Whittington 2006, Jeong et al. 2008a). Megalocytivirus outbreaks are typified by high morbidity and varying degrees of mortality that can approach 100%. Experimental challenge studies using member viruses from each MCV genotype (i.e. ISKNV, RSIV, and TRBIV) have resulted in little to no clinical disease at lower water temperatures (<20°C) compared to warmer water temperatures (>25°C) that have resulted in moribund fish and cumulative mortalities up to 100% (He at al. 2002, Nakajima et al. 2002, Wang et al. 2003, Oh et al. 2006, Jun et al. 2009). However, PCR detection of MCV DNA at cooler temperatures suggests that fish may become infected. Affected fish exhibit nonspecific clinical signs including anorexia, lethargy, increased respiratory effort, gill pallor, darkened coloration, white feces, and internal/external hemorrhages (Fraser et al. 1993, He et al. 2000, Jung & Oh 2000, Chen et al. 2003, Lü et al. 2005, Weber et al. 2009, Sriwanayos et al. 2013). Although notoriously

difficult to isolate in cell culture, MCVs have been associated with systemic infections inducing pathognomonic microscopic lesions, most notably in hematopoietic organs (e.g. anterior kidney and spleen), lamina propria and submucosa of the gastrointestinal tract, liver, and gill (Gibson-Kueh et al. 2003, Weber et al. 2009). Affected cells exhibit progressive cytomegaly that results in the presence of pronounced basophilic intracytoplasmic inclusions. An indirect fluorescent antibody assay has been developed as a confirmatory diagnostic method for RSIV and ISKNV infection in cell cultures and impression smears. Conventional PCR assays can be used to rapidly confirm RSIV and ISKNV from infected tissues or cultures displaying CPE compatible with that of a MCV (i.e. enlarged, rounded, refractile cells) (OIE 2016a).

In this study, we performed phylogenomic analyses to characterize 2 novel MCVs isolated from freshwater ornamental fishes. Additionally, we compared the *in vitro* growth characteristics, microscopic pathology, and ultrastructural pathology of these 2 MCVs to previously reported MCVs. The 2 viruses induced microscopic lesions typically observed in MCV infections, displayed ultrastructural morphology of a MCV, and grouped genetically within the ISKNV genotype TRBIV as a novel clade.

MATERIALS AND METHODS

Archived samples

In 1991, moribund juvenile South American cichlids (oscar *Astronotus ocellatus* and keyhole cichlid *Cleithracara maronii*) from a commercial retail supplier in California were submitted to the Fish Health Laboratory in Davis, CA (FHL-UCD) for virological and histopathological evaluation. Fishes of both species had been recently purchased from a local wholesaler/import facility and were maintained in separate 40 l display tanks prior to exhibiting lethargy, pallor, and mortality within the population. Frozen spent supernatant from the first passage of the South American cichlid iridovirus (SACIV) grown on the bluegill fry cell line in 1991 at the FHL-UCD was shipped on dry ice to the Wildlife and Aquatic Veterinary Disease Laboratory (WAVDL) in Gainesville, FL in 2015. In addition, a second archived MCV isolate grown in tilapia heart cells derived from moribund Florida farm-raised three spot gourami *Trichopodus trichopterus* during epizootics from 1991–1992 (Fraser et al. 1993), hereafter referred to as the three spot gourami iridovirus (TSGIV), was transported on dry ice from the Bronson Animal Disease Diagnostic Laboratory in Kissimmee, FL to the WAVDL in 2015.

The *in vitro* growth characteristics and viral genomic sequencing of the SACIV and TSGIV isolates were carried out at WAVDL. Transmission electron microscopy of infected cultured cells was performed at the University of Texas Medical Branch Electron Microscopy Laboratory (UTMB-EML). Histopathological interpretation was carried out at the FHL-UCD.

Cell culture and virus enrichment

The TSGIV isolate was inoculated onto confluent monolayers of the grunt fin (GF) cells maintained in L15 media with 10% fetal bovine serum and 1% HEPES (4-[2-hydroxyethyl]-1-piperazineethanesulfonic acid) at 28°C. The infected cells were monitored daily for cytopathic effects (CPE) for 14 d post-inoculation. Four 175 cm^2 flasks of GF cells displaying extensive CPE were harvested and subjected to 3 rounds of freeze/thawing prior to clarification of the supernatant by centrifugation at 5520 × *g* for 20 min at 4°C. Pelleted virus was obtained by centrifugation of the clarified supernatant at 100 000 × *g* for 1.25 h at 4°C. The viral pellet was resuspended in 360 µl of animal tissue lysis (ATL) buffer prior to extraction of viral genomic DNA (see below).

Transmission electron microscopy

The TSGIV isolate was propagated in a 75 cm^2 flask of GF cells until CPE was observed. The supernatant from the infected flask was discarded and the monolayer was fixed in 15 ml of modified Karnovsky's fixative (2P+2G, 2% formaldehyde prepared from paraformaldehyde and 2% glutaraldehyde in 0.1 M cacodylate buffer pH 7.4) at room temperature for 1 h. The monolayer was washed in cacodylate buffer, scraped off the flask and pelleted. The pellet was shipped in PBS overnight on ice packs to the University of Texas Medical Branch Department of Pathology Electron Microscopy Laboratory (UTMB-EML). At UTMB-EML, the cell pellet was washed in cacodylate buffer and left in 2P+2G fixative overnight at 4°C. The next day the cell pellet was washed twice in cacodylate buffer, post-fixed in 1% OsO_4 in 0.1 M cacodylate buffer pH 7.4, en bloc stained with 2% aqueous uranyl acetate, dehydrated in ascending concentrations of ethanol, processed through propylene oxide and embedded in Poly/Bed 812 epoxy

plastic (Polysciences). Ultrathin sections were cut on a Leica ULTRACUT EM UC7 ultramicrotome (Leica Microsystems), stained with 0.4% lead citrate, and examined in a JEM-1400 electron microscope (JEOL USA) at 80 kV.

Histopathology

A total of 10 separate juvenile oscars from the 1991 outbreak were fixed in 10% neutral buffered formalin, transected mid-sagittal, processed routinely, and embedded into paraffin with 1 to 2 fish block^{-1}. Sections were cut at 5 µm and stained with hematoxylin and eosin (H&E) for light microscopic examination.

DNA extraction

For formalin-fixed paraffin-embedded (FFPE) tissues, 50 µm sections were cut from blocks using a new microtome blade for each sample to reduce the risk of cross contamination. Qiagen deparaffinization solution, ATL buffer, and Proteinase K were then added to the samples and incubated at 56°C overnight before extraction of DNA was carried out using a DNA FFPE Tissue Kit (Qiagen) according to the manufacturer's instructions. DNA extraction from cell culture supernatant (SACIV) and enriched virus suspended in ATL buffer (TSGIV) was automated with a QIAcube (Qiagen) and a DNeasy Blood and Tissue Kit (Qiagen) using the manufacturer's protocol for animal blood or cells.

Complete genome sequencing, assembly, and annotation

DNA libraries were created using a Nextera XT DNA Kit (Illumina) for SACIV and a TruSeq Kit (Illumina) for TSGIV, then sequenced using a v3 chemistry 600 cycle kit on a MiSeq platform (Illumina). De novo assemblies of the paired-end reads were performed in SPAdes 3.5.0 (Bankevich et al. 2012). The quality of the TSGIV and SACIV assemblies was assessed by mapping reads back to consensus sequences in Bowtie 2 2.1.0 (Langmead & Salzberg 2012), then visually inspecting the alignments in Tablet 1.14.10.20 (Milne et al. 2010).

Open reading frames (ORFs) for the SACIV and TSGIV genomes were predicted using GeneMarkS (http://exon.biology.gatech.edu/) (Besemer et al. 2001), restricting the search to viral sequences. Additional criteria for annotating ORFs were (1) larger than 120 nucleotides, (2) not overlapping with another ORF by more than 25%, and (3) in the case of overlapping ORFs, only the larger ORF was annotated. Gene functions were predicted based on BLASTp searches against the National Center for Biotechnology Information (NCBI) GenBank nonredundant (nr) viruses protein sequence database and NCBI Conserved Domains Database. BLASTn searches of the SACIV and TSGIV ORFs were conducted using the NCBI GenBank nr nucleotide sequence database.

Phylogenetic and genetic analyses

The genomic sequences generated for SACIV and TSGIV were used in 2 separate phylogenetic analyses to demonstrate their relationship to previously characterized MCVs. The 26 iridovirus core genes defined by Eaton et al. (2007) were used to construct a phylogenetic tree for 46 iridoviruses including SACIV and TSGIV (Table 1; Table S1 in the Supplement at www.int-res.com/articles/suppl/d130p011_supp.pdf). Amino acid (AA) sequence alignments for each gene were performed in MAFFT 7 using default parameters (Katoh & Standley 2013) and concatenated using Geneious R10 (Kearse et al. 2012). Maximum likelihood (ML) phylogenetic trees were constructed using Molecular Evolutionary Genetics Analysis (MEGA) version 7.0 (Kumar et al. 2016) using default settings and 1000 bootstraps to determine node support. The same methods were used to construct a ML phylogenetic tree based on the nucleotide sequences of the major capsid protein (MCP) gene to compare the relationships of SACIV and TSGIV to 81 megalocytiviruses from each of the 3 genotypes plus selected outgroups, the threespine stickleback iridovirus and scale drop disease virus (Table S2 in the Supplement). To summarize the genetic distance among the aforementioned 83 MCVs, the MCP nucleotide sequences were aligned using the MAFFT option within the Sequence Demarcation Tool Version 1.2 (Muhire et al. 2014) to generate a sequence identity matrix.

PCR detection of MCVs

To unbiasedly screen FFPE oscar tissue sections for MCV DNA, a pan-MCV primer set was designed to amplify all MCV genotypes (Table 2). The primers were designed to amplify <200 bp given DNA from

Table 1. Summary of the 11 megalocytiviruses (MCVs) and the related scale drop disease virus used in the 26 iridovirus core gene phylogenetic analysis. NA: not applicable; ORFs: open reading frames

Virus (abbreviation)	Host species	MCV genotype and clade	Country of origin	Size (bp)	No. of ORFs	% G+C	Reference
Scale drop disease virus (SDDV)	Giant seaperch *Lates calcarifer*	NA*	Singapore	124 244	129	36.9	de Groof et al. (2015)
Infectious spleen and kidney necrosis virus (ISKNV)	Mandarin fish *Siniperca chuatsi*	ISKNV Clade 1	China	111 362	124	54.8	He et al. (2001)
Infectious spleen and kidney necrosis virus (RSIV-Ku)	Red seabream *Pagrus major*	ISKNV Clade 1	Taiwan	111 154	132	54.7	Shiu et al. (2018)
Turbot reddish body iridovirus (TRBIV)	Turbot *Scophthalmus maximus*	TRBIV Clade 1	China	110 104	115	55.0	Shi et al. (2010)
South American cichlid iridovirus (SACIV)	Keyhole cichlid *Cleithracara maronii*	TRBIV Clade 2	Unknown	111 347	116	56.3	Go et al. (2016)
Three spot gourami iridovirus (TSGIV)	Three spot gourami *Trichopodus trichopterus*	TRBIV Clade 2	United States	111 591	116	56.5	Fraser et al. (1993)
Red seabream iridovirus (RSIV)	Red seabream *Pagrus major*	RSIV Clade 1	Japan	112 414	93	53.0	Kurita et al. (2002)
Giant seaperch iridovirus (GSIV-K1)	Giant seaperch *Lates calcariferi*	RSIV Clade 2	Taiwan	112 565	135	53.0	Wen & Hong (2016)
Orange-spotted grouper iridovirus (OSGIV)	Orange-spotted grouper *Ephinephelus coioides*	RSIV Clade 2	China	112 636	121	54.0	Lü et al. (2005)
Rock bream iridovirus (RBIV-C1)	Rock bream *Oplegnathus fasciatus*	RSIV Clade 2	China	112 333	119	53.0	Zhang et al. (2013)
Rock bream iridovirus (RBIV-KOR-TY1)	Rock bream *Oplegnathus fasciatus*	RSIV Clade 2	Korea	112 080	118	53.0	Do et al. (2004)
Red seabream iridovirus (RSIV RIE12-1)	Red seabream *Pagrus major*	RSIV Clade 2	Japan	112 590	108	53.0	T. Matsuyama et al. (unpubl. data)

*SDDV serves as a distantly related outgroup to members of the genus *Megalocytivirus*

FFPE tissues are typically fragmented (Green & Sambrook 2012). The 26 iridovirus core genes were extracted from the annotated genomic sequences generated in this study for SACIVs and TSGIV (Tables S3 & S4 in the Supplement) as well as for 9 other fully sequenced MCVs available in GenBank (ISKNV, RSIV-Ku, TRBIV, GSIV-K1, OSGIV, RSIV RIE12-1, RBIV-KOR-TY1, RBIV-C1, RSIV) (Tables 1 & S1). For each gene, the nucleotide sequences were aligned in MAFFT 7 (Katoh & Toh 2008) using default settings and the resulting alignments were imported into Geneious R10 (Kearse et al. 2012) to generate a consensus sequence with the threshold set to 100%. The consensus sequences were imported into Primer3 (http://biotools.umassmed.edu/bioapps/primer3_www.cgi) to design pan-MCV primers with the following characteristics: conserved primer binding sites <200 bp apart with a hypervariable region in between to facilitate MCV genotype discrimination by Sanger sequencing.

Reaction volumes for the pan-MCV PCR were 50 µl and consisted of 0.25 µl of Platinum *Taq* DNA Polymerase (Invitrogen), 5.0 µl of 10× PCR Buffer, 2.0 µl of 50 mM $MgCl_2$, 1.0 µl of 10 mM dNTPs, 2.5 µl of 20 µM forward and reverse primers, 32.25 µl of molecular grade water, and 4.5 µl of DNA template. An initial denaturation step of 94°C for 5 min was followed by 40 cycles of a 94°C denaturation step, a 55°C annealing step, and a 72°C extension step, each step run for 30 s, and a final extension step at 72°C for 5 min. PCR products were subjected to electrophoresis in 1% agarose gel stained with ethidium bromide. Amplified products were purified using a QIAquick PCR Purification Kit. The concentration of purified DNA was quantified fluorometrically using a Qubit® 3.0 Fluorometer and dsDNA BR Assay Kit (Life Technolo-

Table 2. Pan-megalocytivirus (MCV) primer set targeting the myristylated membrane protein (ORF 7L in infectious spleen and kidney necrosis virus GenBank accession no. AF371960). The listed amplicon size includes the primers

Primer pair	Primer sequence (5′–3′)	Amplicon size (bp)
MCV-F	CAA CCC CAC GTC CAA AGA	173
MCV-R	ACA TTG CTG GGG CAT GTG	

gies). Purified DNA was sequenced in both directions on an ABI 3130 platform (Applied Biosystems).

DNA from the SACIV and TSGIV isolates were tested against the pan-MCV PCR. In addition, the PCR assay was tested using DNA extracted from (1) freshly frozen tissues: splenic tissue of a moribund Florida pompano *Trachinotus carolinus* infected with RSIV (T. B. Waltzek & R. P. Yanong unpubl. data) and hepatic tissue from a moribund ram cichlid infected with ISKNV (T. B. Waltzek unpubl. data) and (2) FFPE tissues: TRBIV Clade 2-infected oscar (Go et al. 2016), ISKNV-infected Nile tilapia *Oreochromis niloticus* (Subramaniam et al. 2016), and RSIV-infected Florida pompano (Table 3). To test for any cross reaction between other members of the subfamily *Alphairidovirinae*, the pan-MCV primer set was tested against ranavirus isolated from pallid sturgeon *Scaphirhynchus albus* (Waltzek et al. 2014) and lymphocystivirus-positive tissues obtained from a copperband butterflyfish *Chelmon rostratus* (Clark et al. 2018), respectively.

RESULTS

Cell culture and virus enrichment

The GF cells displayed CPE (enlargement, rounding, and refractility) within 96 h of being infected with the TSGIV isolate (Fig. 1A,B). Complete CPE was observed by Day 10 post-infection (pi), in which most cells were affected but remained attached to the monolayer (Fig. 1C,D). No CPE was observed following inoculation of GF cells with the SACIV isolate.

Transmission electron microscopy

Viral particles from the TSGIV inoculation were observed within the cytoplasm of GF cells, occasionally arranged in paracrystalline arrays (Fig. 2A). Intracytoplasmic viral particles were unenveloped, had hexagonal nucleocapsids, and displayed electron-dense cores, cores with medium electron densities, or electron-lucent cores (Fig. 2B). The mean diameter (±SD) of the viral particles from opposite vertices was 144 ± 10 nm (n = 20) and 120 ± 7 nm (n = 20) from opposite faces. Although no enveloped virions were observed intracellularly or extracellularly, virions were observed within cellular blebs and in membrane-bound intracytoplasmic vesicles separated from infected cells (Fig. 2A). The GF cells innoculated with the SACIV were not submitted for transmission electron microscopy as CPE was not observed.

Histopathology

Of the 10 sections of oscars that were examined, 6 displayed intravascular or hematopoietic cytomegalic cells characterized by basophilic, granular, intracytoplasmic inclusions within various organs that were especially prominent in the anterior kidney, spleen, and intestinal mucosa and submucosa (Fig. 3). In one section, approximately 50% of the lymphomyeloid cells of the anterior kidney were affected (Fig. 3A,B). Cytomegalic cells displaying basophilic inclusions were also noted within the pulp cavity of the teeth, oropharyngeal submucosa, stomach, posterior kidney (renal interstitial hematopoietic tissue and glomeruli), branchial lamellar capillaries, pseudobranch, ocular rete mirabile, pancreas, gonadal interstitium, coelomic cavity membranes, skeletal and cardiac muscle, cartilage, and connective tissue regardless of location.

Complete genome sequencing, assembly, and annotation

For SACIV, the de novo assembly of 7 721 890 paired-end reads produced a contiguous consensus sequence of 111 347 bp with a G+C content of 56.3% (Table 1). A total of 2 421 194 reads (31.35%) aligned at a mean coverage of 4931 reads nucleotide^{-1}. For TSGIV, the de novo assembly of 3 229 544 paired-end reads produced a consensus sequence of 111 591 bp with a G+C content of 56.5%. A total of 445 855 reads (13.81%) aligned at a mean coverage of 1178 reads nucleotide^{-1}. Both genomes displayed 116 ORFs (see Tables S3 & S4); the complete genomes of SACIV and TSGIV have been deposited in GenBank with the accession nos. MG570131 and MG570132, respectively.

Table 3. Iridovirus samples tested against the conventional pan-MCV PCR assay. FFPE: Formalin-fixed paraffin-embedded; ISKNV: infectious spleen and kidney necrosis virus; MCV: Megalocytivirus; NA: not applicable; RSIV: red seabream iridovirus; TRBIV: turbot reddish body iridovirus

Host common name	Host species	MCV genotype	Material	Year collected	Origin	Reference
Copperband butterflyfish	*Chelmon rostratus*	NA[a]	Fresh, frozen fin	2015	Florida, USA	Clark et al. (2018)
Florida pompano	*Trachinotus carolinus*	RSIV	FFPE	2014	Dominican Republic	T. B. Waltzek & R. P. Yanong (unpubl. data)
Florida pompano	*Trachinotus carolinus*	RSIV	Fresh, frozen spleen	2016	Dominican Republic	T. B. Waltzek & R. P. Yanong (unpubl. data)
Keyhole cichlid	*Cleithracara maronii*	TRBIV	Viral isolate	1991	California, USA	Go et al. (2016)
Nile tilapia	*Oreochromis niloticus*	ISKNV	FFPE	2012	Idaho, USA	Subramaniam et al. (2016)
Oscar	*Astronotus ocellatus*	TRBIV	FFPE	1991	California, USA	Go et al. (2016)
Oscar	*Astronotus ocellatus*	TRBIV	Viral isolate	1991	California, USA	Go et al. (2016)
Pallid sturgeon	*Scaphirhynchus albus*	NA[b]	Viral isolate	2009	Missouri, USA	Waltzek et al. (2014)
Ram cichlid	*Mikrogeophagus ramirezi*	ISKNV	Fresh, frozen liver	2015	Florida, USA	T. B. Waltzek (unpubl. data)
Three spot gourami	*Trichopodus trichopterus*	TRBIV	Viral isolate	1991	Florida, USA	Fraser et al. (1993)

[a]Lymphocystivirus-infected sample; [b]Ranavirus isolate

BLAST searches for the SACIV and TSGIV genomes revealed they share the highest AA identity to each other for 114/116 ORFs (Tables S3 & S4). In total, 75 ORFs displayed 100% nucleotide identity to each other, 11 ORFs displayed 1 or more synonymous changes, and 30 ORFs displayed 1 or more non-synonymous changes. Five of the 116 ORFs differed in size between SACIV and TSGIV; 3 encoded hypothetical proteins and the other 2 encoded a laminin-type epidermal growth factor and transcription factor SII. Both SACIV and TSGIV encode a unique truncated paralog of the MCP gene (ORF 6L) located immediately upstream of the full length parent gene (ORF 7L).

Phylogenetic and genetic analyses

Phylogenetic analyses based on the 26 iridovirus core genes and MCP gene revealed SACIV and TSGIV form a well-supported clade (hereafter referred to as the TRBIV Clade 2) as the sister group to TRBIV Clade 1 (Figs. 4 & 5). The MCP nucleotide identity of the TRBIV Clade 2 MCVs compared to each other was 99.9 to 100%, 95.9 to 96.7% identity when compared to TRBIV Clade 1 MCVs, and 92.4 to 93.6% identity when compared to members of the other 2 genotypes (i.e. ISKNV, RSIV) (Table S5).

PCR detection of MCVs

Primers (MCV-F and MCV-R) that met the specified criteria were generated against ORF 8L, the myristylated membrane protein, and produced a 173 bp amplicon (including primers) (Fig. 6, Table 2). A single band was observed from DNA extracted from isolates of SACIV and TSGIV, freshly frozen tissue infected with ISKNV and RSIV, and FFPE tissue infected with ISKNV, RSIV, and TRBIV. Sequencing of amplicons confirmed the expected genotype including TRBIV Clade 2 for the oscar, keyhole cichlid, and three spot gourami samples. No cross reactivity was detected when the assay was tested against a ranavirus isolate and lymphocystivirus-infected tissues.

DISCUSSION

In this investigation, we reported the first complete genome sequences for TRBIV Clade 2 MCVs (SACIV and TSGIV) isolated from cultured South American cichlids and three spot gourami during outbreaks in

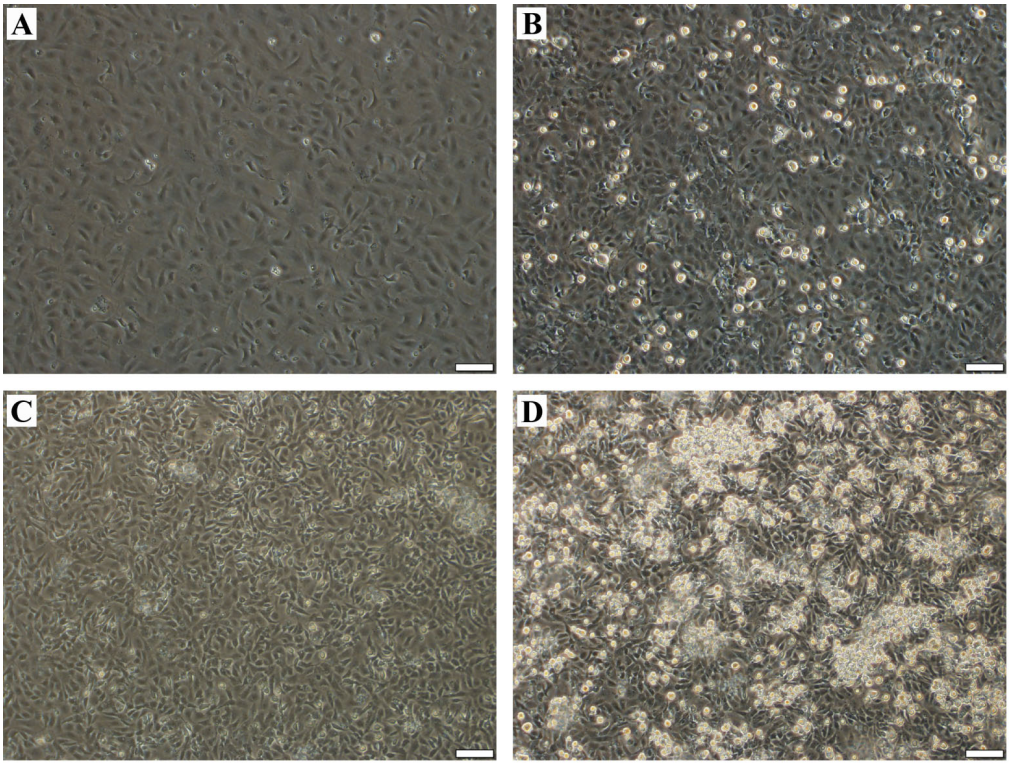

Fig. 1. Microscopic examination of *in vitro* growth characteristics of three spot gourami iridovirus in the grunt fin cell line at 28°C. (A) Control flask 96 h post-infection (pi); (B) infected flask 96 hpi showing rounded, enlarged, refractile cells; (C) control flask on Day 10 pi; (D) infected flask on Day 10 pi showing aggregates of rounded, enlarged, refractile cells. Scale bars = 50 µm

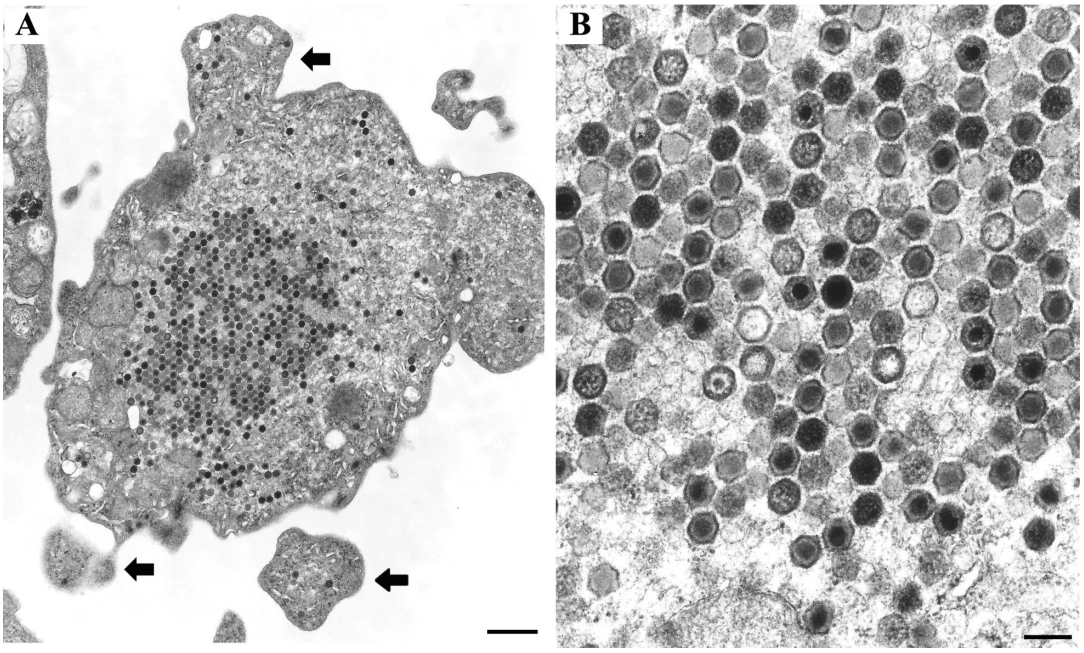

Fig. 2. (A) Transmission electron photomicrograph of a grunt fin cell infected with three spot gourami iridovirus. A paracrystalline array of virus particles is located in the cytoplasm with low numbers of virus particles present in the cellular blebs and membrane-bound intracytoplasmic vesicles apparently separated from the infected cell (see arrows). Scale bar = 1 µm. (B) At higher magnification, virus particles display hexagonal nucleocapsids, and possess electron-dense cores, cores of medium electron density, and electron-lucent cores. Scale bar = 200 nm

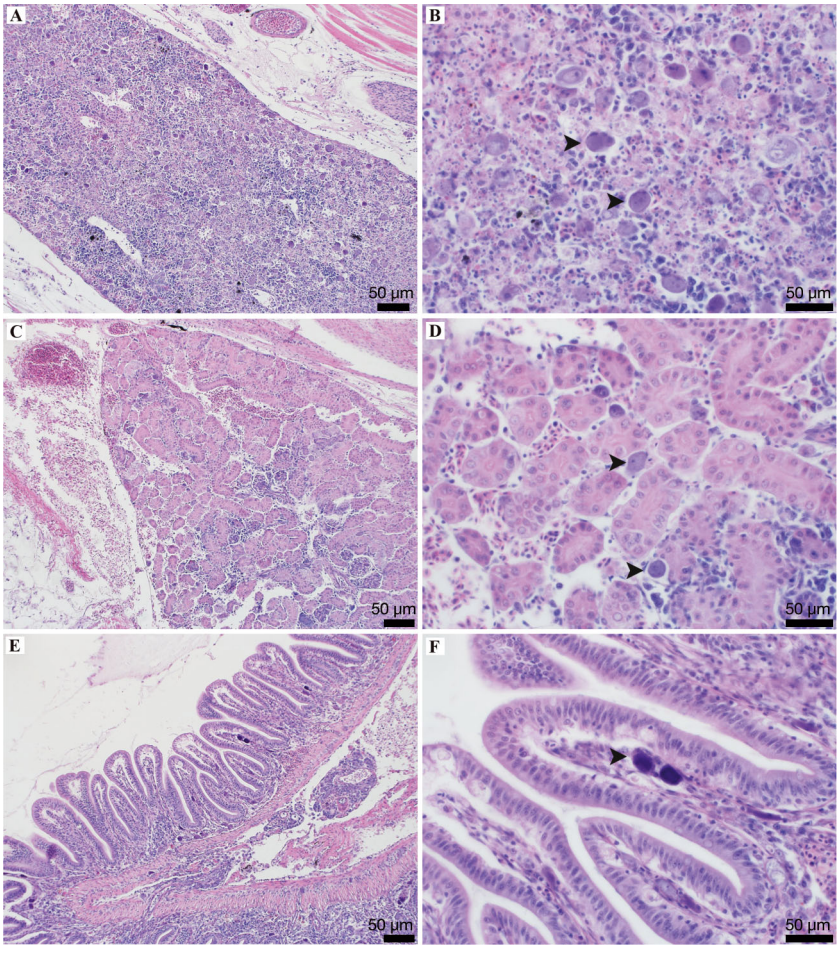

Fig. 3. Microscopic examination of cytomegalic cells (arrowheads) and lesions in infected oscar *Astronotus ocellatus*. H&E stain. Cytomegalic cells with basophilic intracytoplasmic inclusions are located (A,B) in the hematopoietic tissue along with necrotic cells, pyknotic and karyorrhectic debris in the anterior kidney, (C,D) in the interstitium between renal tubules of the posterior kidney, and (E,F) in the lamina propria of the intestine supporting an intact and uninfected muscosal epithelium. Scale bars = 50 µm

the early 1990s (Fraser et al. 1993, Go et al. 2016). Go et al. (2016) recently characterized TRBIV Clade 2, based on the MCP and ATPase gene sequences, from earlier outbreaks involving angelfish *Pterophyllum scalare* imported into Canada from Asia (Schuh & Shirley 1990) and dwarf gourami *Trichogaster lalius* imported into Australia from Asia (Anderson et al. 1993). It is unclear why the TRBIV Clade 2 MCVs have not been detected in the international ornamental fish trade since the 1991 SACIV outbreak in California and the 1991 and 1992 TSGIV outbreaks in Florida (Fraser et al. 1993, Go et al. 2016). Recently, outbreaks in freshwater ornamental fishes have been attributed to ISKNV Clade 1 MCVs and outbreaks in marine ornamental fishes have been due to ISKNV Clade 2 MCVs (Weber et al. 2009, Sriwanayos et al. 2013, Go et al. 2016, Dong et al. 2017). The pan-MCV PCR assay described here could prove to be a valuable tool in future surveillance efforts aimed at rapidly identifying the MCV genotype from isolates and fresh or fixed tissues following additional optimization and validation (Table 2).

The most recent detection of a TRBIV Clade 2 MCV involved a high-mortality event that occurred on a Taiwanese farm rearing rock bream for food (Huang et al. 2011). Similarly, TRBIV Clade 1 MCVs have impacted turbot *Scophthalmus maximus* and other flatfish species reared for food in China and Korea (Do et al. 2005a,b, Shi et al. 2010). The finding of related TRBIV MCVs in both freshwater ornamental fishes and marine food fish species is not surprising given the low host specificity of MCVs (Kawato et al. 2017). Experimental challenge studies have shown that ISKNV Clade 1 MCVs derived from a freshwater fish (pearl gourami *Trichogaster leeri*) can induce lethal disease in a marine food-fish species

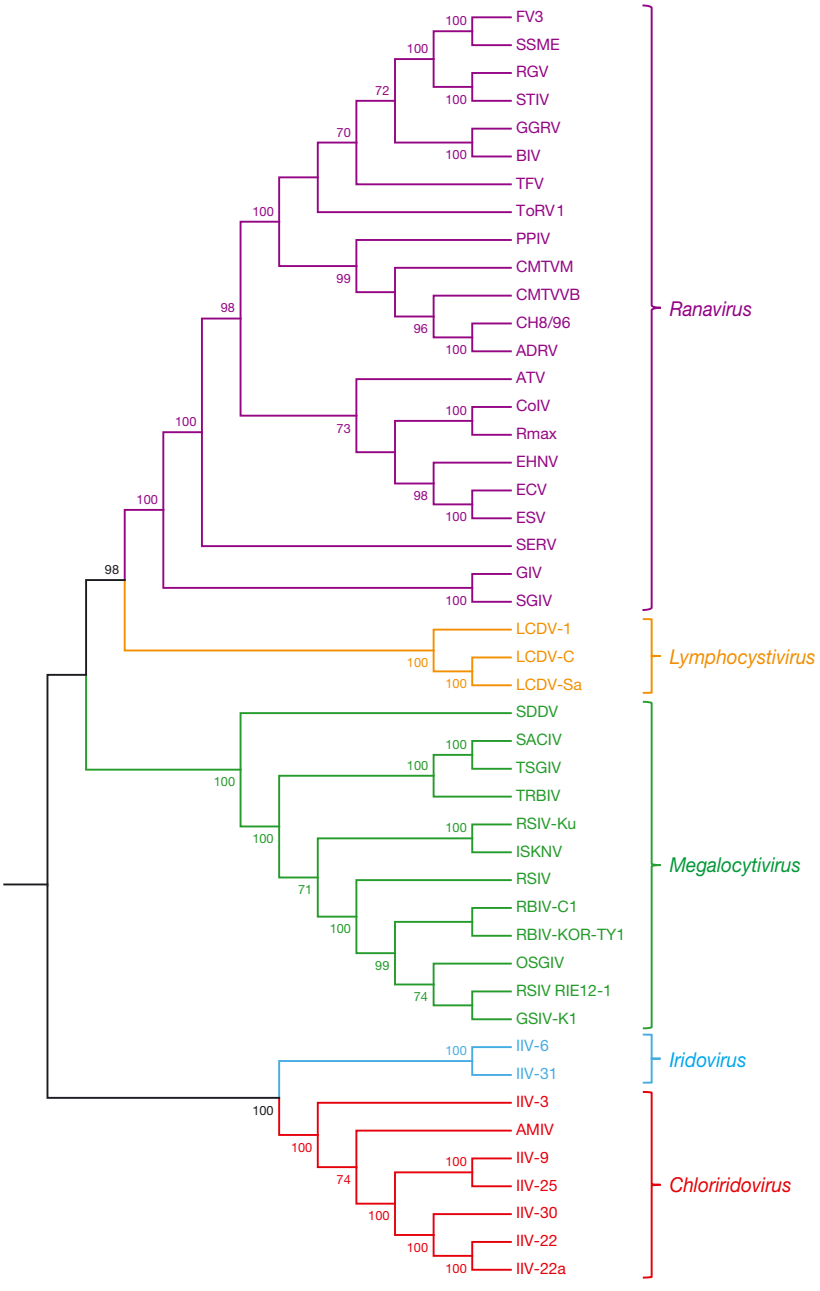

Fig. 4. Relationship of South American cichlid iridovirus and three spot gourami iridovirus to the other members of the family *Iridoviridae* based on 26 iridovirus core genes. The maximum likelihood tree was created using 1000 bootstraps in MEGA 7 and bootstrap support values >70 were included. Branch lengths are based on the number of inferred substitutions, as indicated by the scale. Refer to Table S1 in the Supplement for virus abbreviations, and Tables S3 & S4 for the list of 26 iridovirus core genes

rock bream (Jeong et al. 2008a). Dwarf gourami can transmit the dwarf gourami iridovirus (ISKNV Clade 1) by cohabitation with Murray cod *Maccullochella peelii*, a highly valued sport and food fish in Australia (Go & Whittington 2006). Finally, there is evidence that ISKNV Clade 1 has resulted in concurrent outbreaks in Nile tilapia *Oreochromis niloticus* reared for food and angelfish reared for the ornamental trade on the same farm (Subramaniam et al. 2016). Given that MCVs appear capable of readily crossing environmental and host boundaries, stringent biosecurity practices should be implemented when rearing highly susceptible ornamental species (e.g. angelfish and gourami) alongside susceptible food fishes (e.g. rock bream and Nile tilapia) (Jeong et al. 2008b, Subramaniam et al. 2016).

Genome sizes of SACIV and TSGIV, % G+C, ORF number and orientation are consistent with those reported for members of the genus *Megalocytivirus* (Chinchar et al. 2009, 2017) (Table 1). Phylogenetic analyses based on the 26 iridovirus core genes and MCP gene highly supported SACIV and TSGIV as a novel clade (TRBIV Clade 2) and sister group to the TRBIV Clade 1 MCVs (Figs. 4 & 5). Similarly, genetic analyses confirmed the close relationship of TRBIV Clade 2 MCVs to each other and to members of TRBIV Clade 1 (see Table S5 in the Supplement).

A molecular synapomorphy (i.e. shared derived feature) for the TRBIV Clade 2 MCVs is the presence of a truncated paralog of the MCP gene (ORF 6L) located immediately upstream of the full length parent gene (ORF 7L; Tables S3 & S4). To our knowledge, this is the only report of a duplicated MCP gene in an iridovirus or the related nucleocytoplasmic large DNA viruses. The MCP paralog likely arose through a gene duplication event, and if expressed, its function could be to increase viral antigenic diversity. Gene duplication events are a common mechanism pathogens employ to increase antigenic diversity to evade host immune responses (Pays et al. 1981, Ferreira et al. 2004). The iridovirus MCP is the predominant structural component of the virion and is thought to be the most important protective antigen (Caipang et al. 2006, Shinmoto et al. 2009, Fu et al. 2014).

Histopathological examination of oscar tissue sections infected with SACIV revealed microscopic lesions comparable to those previously reported in

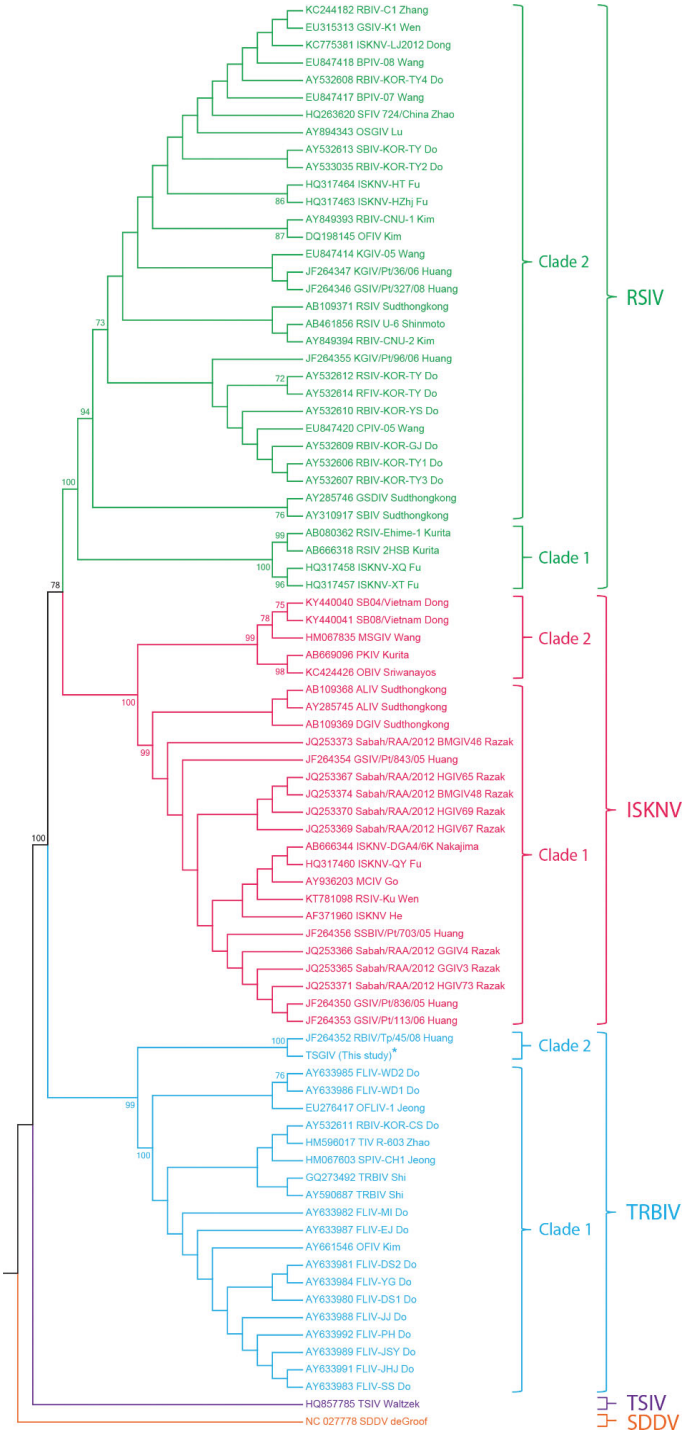

Fig. 5. Cladogram (adapted from Go et al. 2016) illustrating the relationship of megalocytiviruses based on the major capsid protein (MCP) gene. The maximum likelihood tree was created using 1000 bootstraps and support values >70 were included. Branch lengths are based on the number of inferred substitutions as indicated by the scale. *The TLMV, PSMV, and SACIV sequences have 100% nucleotide sequence identity to TSGIV (this study) and thus were not included in the MCP phylogenetic analysis. Refer to Table S2 in the Supplement for virus abbreviations

three spot gourami infected with TSGIV (Fraser et al. 1993) and typical of MCVs (Gibson-Kueh et al. 2003, Weber et al. 2009). Numerous cytomegalic cells characterized by basophilic granular intracytoplasmic inclusions were observed systematically and were especially prominent in the anterior kidney, spleen, and intestinal lamina propria and submucosa. Cytomegalic cells in the SACIV-infected tissues were not recognized in epithelial cells of lesioned tissues and may be of a mesenchymal or lymphomyeloid origin as previously described (Weber et al. 2009, Subramaniam et al. 2016). Additional research is needed to better define MCV histogenesis.

Although originally isolated in tilapia heart cells (Fraser et al. 1993), the TSGIV isolate produced the expected CPE (i.e. cellular rounding and enlargement) for MCVs (e.g. RSIV) grown in GF cells (Kawato et al. 2017, our Fig. 1). The SACIV did not display CPE in the GF cell line, which may have been due to the storage of this sample at –80°C since 1991 (Go et al. 2016) compared to the TSGIV sample that was stored in liquid nitrogen since 1991 (Fraser et al. 1993). Additionally, the first passage SACIV supernatant used in this study was derived from a bluegill fry culture that displayed minimal CPE, suggesting a low viral titer (Go et al. 2016). Thus, the presumed low viral titer and long-term preservation of the SACIV supernatant may have affected our ability to revive it.

Ultrastructural examination of TSGIV-infected GF cells revealed unenveloped, hexagonal nucleocapsids and electron-dense cores within the cytoplasm, sometimes arranged in paracrystalline arrays (Fig. 2) which were consistent with previous MCV reports (Weber et al. 2009, Kawato et al. 2017). In contrast to iridoviruses from related genera (e.g. ranaviruses and lymphocystiviruses) that acquire an outer envelope as they bud through the host cell plasma membrane, TSGIV particles were not observed budding from infected GF cells. In TSGIV-infected GF cells, virus particles were observed in cellular blebs (Fig. 2A), similar to RSIV-infected GF cells that undergo apoptosis and generate apoptotic body-like vesicles that are phagocytized by neighboring cells (Imajoh et al. 2004). Our review of previous MCV reports did not reveal a single convincing study demonstrating that MCVs acquire an outer envelope by budding through the host cell membrane during virion morphogenesis (Fraser et al. 1993, He et al. 2000, Chen et al. 2003, Gibson-Kueh et al. 2003, Sriwanayos et al. 2013). Thus, one might postulate that TSGIV, like other MCVs, do not employ envelope proteins to initiate receptor mediated endocytosis for

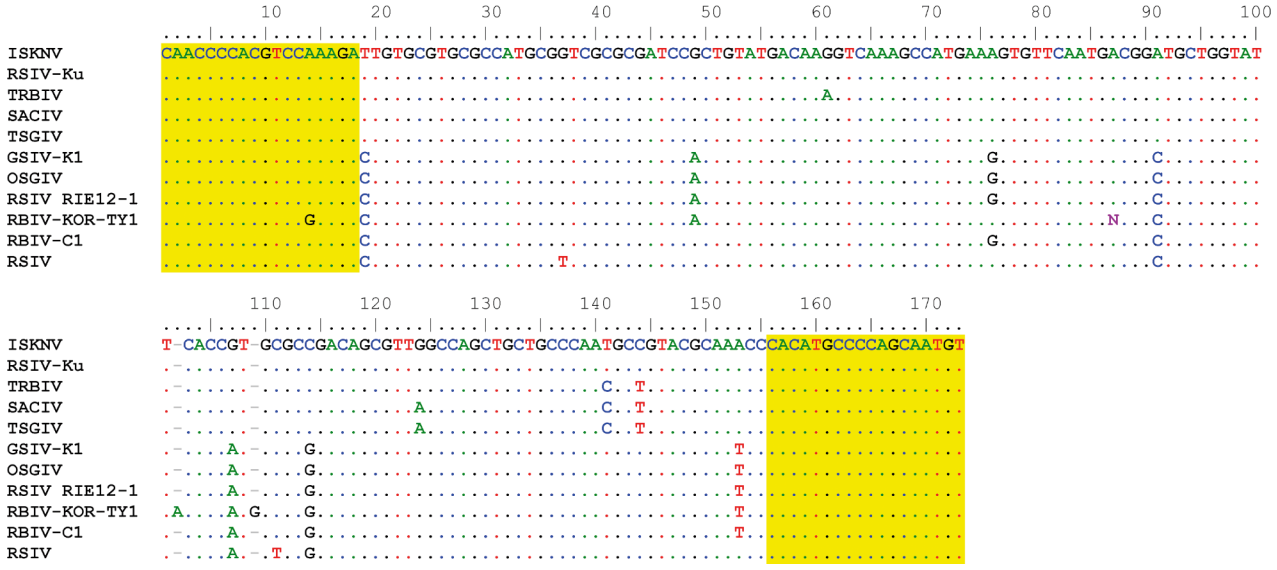

Fig. 6. Nucleotide sequence alignment of *Infectious spleen and kidney necrosis virus* (ISKNV; ISKNV Clade 1), red seabream iridovirus (RSIV-Ku; ISKNV Clade 1), turbot reddish body iridovirus (TRBIV; TRBIV Clade 1), South American cichlid iridovirus (SACIV; TRBIV Clade 2), three spot gourami iridovirus (TSGIV; TRBIV Clade 2), giant seaperch iridovirus (GSIV-K1; RSIV Clade 2), orange spotted grouper iridovirus (OSGIV; RSIV Clade 2), red seabream iridovirus (RSIV RIE12-1; RSIV Clade 2), rock bream iridovirus (RBIV-KOR-TY1; RSIV Clade 2), rock bream iridovirus (RBIV-C1; RSIV Clade 2) and red seabream iridovirus (RSIV; RSIV Clade 1) for a 173 bp region of the myristylated membrane protein gene (ORF 7L in ISKNV). Highlighted regions represent the pan-MCV primer (MCV-F and MCV-R) binding sites. Refer to Table 1 for additional details on these MCVs, and Table S1 in the Supplement for GenBank accession nos.

cellular entry as has been demonstrated in the ranavirus species *Frog virus 3* and *Singapore grouper iridovirus* (Gendrault et al. 1981, Wang et al. 2014). Interestingly, *in vitro* studies of ISKNV suggest it enters mandarin fish fry cells through caveolar endocytosis (Guo et al. 2012, Jia et al. 2013). More studies are needed to determine how other MCVs such as TSGIV enter (e.g. phagocytosis, caveolar endocytosis) and exit (e.g. apoptotic blebs, cell lysis) host cells.

The growth of TSGIV in GF cells (Fig. 1) will permit future challenge studies to unequivocally determine the role of TRBIV Clade 2 MCVs in disease (i.e. fulfillment of Koch's postulates). The establishment of an effective challenge model will permit the development of effective MCV mitigation strategies including testing the effect of environmental manipulation (e.g. temperature and density) and vaccination. Although a formalin-inactivated vaccine has reduced the impact of RSIV disease on Japanese food fish mariculture, its economic viability and effectiveness against other MCV genotypes infecting ornamental fishes has yet to be determined (Nakajima et al. 1997, 1999, Kawato et al. 2017).

Acknowledgements. We thank P. M. Thompson for his technical assistance throughout the project, J. Shelly for providing samples, and J. Go for reviewing the manuscript.

LITERATURE CITED

Anderson IG, Prior HC, Rodwell BJ, Harris GO (1993) Iridovirus-like virions in imported dwarf gourami (*Colisa lalia*) with systemic amoebiasis. Aust Vet J 70: 66–67

Bankevich A, Nurk S, Antipov D, Gurevich AA and others (2012) SPAdes: a new genome assembly algorithm and its applications to single-cell sequencing. J Comput Biol 19:455–477

Besemer J, Lomsadze A, Borodovsky M (2001) GeneMarkS: a self-training method for prediction of gene starts in microbial genomes. Implications for finding sequence motifs in regulatory regions. Nucleic Acids Res 29: 2607–2618

Caipang CM, Takano T, Hirono I, Aoki T (2006) Genetic vaccines protect red seabream, *Pagrus major*, upon challenge with red seabream iridovirus (RSIV). Fish Shellfish Immunol 21:130–138

Chen XH, Lin KB, Wang XW (2003) Outbreaks of an iridovirus disease in maricultured large yellow croaker, *Larimichthys crocea* (Richardson), in China. J Fish Dis 26:615–619

Chinchar VG, Hyatt A, Miyazaki T, Williams T (2009) Family *Iridoviridae*: poor viral relations no longer. Curr Top Microbiol Immunol 328:123–170

Chinchar VG, Hick P, Ince IA, Jancovich JK and others (2017) ICTV virus taxonomy profile: *Iridoviridae.* J Gen Virol 98:890–891

Clark AS, Behringer DC, Small JM, Waltzek TB (2018) Partial validation of a TaqMan real-time quantitative PCR assay for the detection of *Panulirus argus* virus 1. Dis Aquat Org 129:193–198

de Groof A, Guelen L, Deijs M, van der Wal Y and others (2015) A novel virus causes scale drop disease in *Lates calcarifer*. PLOS Pathog 11:e1005074

Do JW, Moon CH, Kim HJ, Ko MS and others (2004) Complete genomic DNA sequence of rock bream iridovirus. Virology 325:351–363

Do JW, Cha SJ, Kim JS, An EJ and others (2005a) Phylogenetic analysis of the major capsid protein gene of iridovirus isolates from cultured flounders *Paralichthys olivaceus* in Korea. Dis Aquat Org 64:193–200

Do JW, Cha SJ, Kim JS, An EJ and others (2005b) Sequence variation in the gene encoding the major capsid protein of Korean fish iridoviruses. Arch Virol 150:351–359

Dong HT, Jitrakorn S, Kayansamruaj P, Pirarat N and others (2017) Infectious spleen and kidney necrosis disease (ISKND) outbreaks in farmed barramundi (*Lates calcarifer*) in Vietnam. Fish Shellfish Immunol 68:65–73

Eaton HE, Metcalf J, Penny E, Tcherepanov V, Upton C, Brunetti CR (2007) Comparative genomic analysis of the family *Iridoviridae*: re-annotating and defining the core set of iridovirus genes. Virol J 4:11

Ferreira MU, da Silva Nunes M, Wunderlich G (2004) Antigenic diversity and immune evasion by malaria parasites. Clin Diagn Lab Immunol 11:987–995

Fraser WA, Keefe TJ, Bolon B (1993) Isolation of an iridovirus from farm-raised gouramis (*Trichogaster trichopterus*) with fatal disease. J Vet Diagn Invest 5:250–253

Fu X, Li N, Lin Q, Guo H, Zhang D, Liu L, Wu S (2014) Protective immunity against infectious spleen and kidney necrosis virus induced by immunization with DNA plasmid containing *mcp* gene in Chinese perch *Siniperca chuatsi*. Fish Shellfish Immunol 40:259–266

Gendrault JL, Steffan AM, Bingen A, Kirn A (1981) Penetration and uncoating of frog virus 3 in cultured rat Kupffer cells. Virology 112:375–384

Gibson-Kueh S, Netto P, Ngoh-Lim GH, Chang SF and others (2003) The pathology of systemic iridoviral disease in fish. J Comp Pathol 129:111–119

Go J, Whittington R (2006) Experimental transmission and virulence of a megalocytivirus (Family *Iridoviridae*) of dwarf gourami (*Colisa lalia*) from Asia in Murray cod (*Maccullochella peelii peelii*). Aust Aquacult 258:140–149

Go J, Waltzek TB, Subramaniam K, Yun SC and others (2016) Detection of infectious spleen and kidney necrosis virus (ISKNV) and turbot reddish body iridovirus (TRBIV) from archival ornamental fish samples. Dis Aquat Org 122:105–123

Green MR, Sambrook J (2012) Molecular cloning, a laboratory manual, 4th edn. Cold Spring Harbor Laboratory Press, Cold Spring Harbor, NY

Guo CJ, Wu YY, Yang LS, Yang XB and others (2012) Infectious spleen and kidney necrosis virus (a fish iridovirus) enters mandarin fish fry cells via caveola-dependent endocytosis. J Virol 86:2621–2631

He JG, Wang SP, Zeng K, Huang ZJ, Chan S (2000) Systemic disease caused by an iridovirus-like agent in cultured mandarinfish, *Sinipercca chuatsi* (Basilewsky), in China. J Fish Dis 23:219–222

He JG, Deng M, Weng SP, Li Z and others (2001) Complete genome analysis of the mandarin fish infectious spleen and kidney necrosis iridovirus. Virology 291:126–139

He JG, Zeng K, Weng SP, Chan SM (2002) Experimental transmission, pathogenicity and physical-chemical properties of infectious spleen and kidney necrosis virus (ISKNV). Aquaculture 204:11–24

Huang SM, Tu C, Tseng CH, Huang CC, Chou CC, Kuo HC, Chang SK (2011) Genetic analysis of fish iridoviruses isolated in Taiwan during 2001-2009. Arch Virol 156: 1505–1515

Imajoh M, Sugiura H, Oshima S (2004) Morphological changes contribute to apoptotic cell death and are affected by caspase-3 and caspase-6 inhibitors during red sea bream iridovirus permissive replication. Virology 322:220–230

Jeong JB, Jun LJ, Yoo MH, Kim MS, Komisar JL, Jeong HD (2003) Characterization of the DNA nucleotide sequences in the genome of red sea bream iridoviruses isolated in Korea. Aquaculture 220:119–133

Jeong JB, Cho HJ, Jun LJ, Hong SH, Chung J, Jeong HD (2008a) Transmission of iridovirus from freshwater ornamental fish (pearl gourami) to marine fish (rock bream). Dis Aquat Org 82:27–36

Jeong JB, Kim HY, Jun LJ, Lyu JH, Park NG, Kim JK, Jeong HD (2008b) Outbreaks and risks of infectious spleen and kidney necrosis virus disease in freshwater ornamental fishes. Dis Aquat Org 78:209–215

Jia KT, Wu YY, Liu ZY, Mi S and others (2013) Mandarin fish caveolin 1 interaction with major capsid protein of infectious spleen and kidney necrosis virus and its role in early stages of infection. J Virol 87:3027–3038

Jun LJ, Jeong JB, Kim JH, Nam JH and others (2009) Influence of temperature shifts on the onset and development of red sea bream iridoviral disease in rock bream *Oplegnathus fasciatus*. Dis Aquat Org 84:201–208

Jung SJ, Oh MF (2000) Iridovirus-like infection associated with high mortalities of striped beakperch, *Oplegnathus fasciatus* (Temminck et Schlegel), in southern coastal areas of the Korean peninsula. J Fish Dis 23:223–226

Katoh K, Standley DM (2013) MAFFT multiple sequence alignment software version 7: improvements in performance and usability. Mol Biol Evol 30:772–780

Katoh K, Toh H (2008) Recent developments in the MAFFT multiple sequence alignment program. Brief Bioinform 9: 286–298

Kawato Y, Subramaniam K, Nakajima K, Waltzek T, Whittington R (2017) Iridoviral diseases: red sea bream iridovirus and white sturgeon iridovirus. In: Woo PTK, Cipriano RC (eds) Fish viruses and bacteria: pathobiology and protection. CABI Publishing, Wallingford, p 147–159

Kearse M, Moir R, Wilson A, Stones-Havas S and others (2012) Geneious Basic: an integrated and extendable desktop software platform for the organization and analysis of sequence data. Bioinformatics 28:1647–1649

Kumar S, Stecher G, Tamura K (2016) MEGA7: molecular evolutionary genetics analysis version 7.0 for bigger datasets. Mol Biol Evol 33:1870–1874

Kurita J, Nakajima K, Hirono I, Aoki T (2002) Complete genome sequencing of red sea bream iridovirus (RSIV). Fish Sci 68:1113–1115

Langmead B, Salzberg SL (2012) Fast gapped-read alignment with Bowtie 2. Nat Methods 9:357–359

Leibovitz L, Riis RC (1980) A viral disease of aquarium fish. J Am Vet Med Assoc 177:414–416

Lü L, Zhou SY, Chen C, Weng SP, Chan SM, He JG (2005) Complete genome sequence analysis of an iridovirus isolated from the orange-spotted grouper, *Epinephelus coioides*. Virology 339:81–100

Milne I, Bayer M, Cardle L, Shaw P, Stephen G, Wright F, Marshall D (2010) Tablet—next generation sequence assembly visualization. Bioinformatics 26:401–402

Muhire BM, Varsani A, Martin DP (2014) SDT: a virus classification tool based on pairwise sequence alignment and identity calculation. PLOS ONE 9:e108277

Nakajima K, Kurita J (2005) Red sea bream iridoviral disease. Uirusu 55(Spec Issue 3):115–125

Nakajima K, Maeno Y, Kurita J, Inui Y (1997) Vaccination against red sea bream iridoviral disease in red sea bream. Fish Pathol 32:205–209

Nakajima K, Maeno Y, Honda A, Yokohama K, Tooriyama T, Manabe S (1999) Effectiveness of a vaccine against red sea bream iridoviral disease in a field trial test. Dis Aquat Org 36:73–75

Nakajima K, Ito T, Kurita J, Kawakami H and others (2002) Effectiveness of a vaccine against red sea bream iridoviral disease in various cultured marine fish under laboratory conditions. Fish Pathol 37:90–91

Oh MJ, Kitamura S, Kim WS, Park MK, Jung SJ, Miyadai T, Ohtani M (2006) Susceptibility of marine fish species to a megalocytivirus, turbot iridovirus, isolated from turbot, *Psetta maximus* (L.). J Fish Dis 29:415–421

OIE (World Organisation for Animal Health) (2016a) Red sea bream iridoviral disease. In: Manual of diagnostic tests for aquatic animals. OIE, Paris. www.oie.int/index.php?id=2439&L=0&htmfile=chapitre_rsbid.htm

OIE (2016b) Disease of fish. In: Aquatic animal health code. OIE, Paris. www.oie.int/en/standard-setting/aquatic-code/access-online/

Pays E, Van Meirvenne N, Le Ray D, Steinert M (1981) Gene duplication and transposition linked to antigenic variation in *Trypanosoma brucei*. Proc Natl Acad Sci USA 78: 2673–2677

Schuh JC, Shirley IG (1990) Viral hematopoietic necrosis in an angelfish (*Pterophyllum scalare*). J Zoo Wildl Med 21: 95–98

Shi CY, Jia KT, Yang B, Huang J (2010) Complete genome sequence of a Megalocytivirus (family *Iridoviridae*) associated with turbot mortality in China. Virol J 7:159

Shinmoto H, Taniguchi K, Ikawa T, Kawai K, Oshima S (2009) Phenotypic diversity of infectious red sea bream iridovirus isolates from cultured fish in Japan. Appl Environ Microbiol 75:3535–3541

Shiu JY, Hong JR, Ku CC, Wen CM (2018) Complete genome sequence and phylogenetic analysis of megalocytivirus RSIV-Ku: a natural recombination infectious spleen and kidney necrosis virus. Arch Virol 163:1037–1042

Song JY, Kitamura SI, Jung SJ, Miyadai T and others (2008) Genetic variation and geographic distribution of megalocytiviruses. Int J Microbiol 46:29–33

Sriwanayos P, Francis-Floyd R, Stidworthy MF, Petty BD, Kelley K, Waltzek TB (2013) Megalocytivirus infection in orbiculate batfish *Platax orbicularis.* Dis Aquat Org 105: 1–8

Subramaniam K, Gotesman M, Smith CE, Steckler NK, Kelley KL, Groff JM, Waltzek TB (2016) Megalocytivirus infection in cultured Nile tilapia *Oreochromis niloticus.* Dis Aquat Org 119:253–258

Sudthongkong C, Miyata M, Miyazaki T (2002a) Iridovirus disease in two ornamental tropical freshwater fishes: African lampeye and dwarf gourami. Dis Aquat Org 48: 163–173

Sudthongkong C, Miyata M, Miyazaki T (2002b) Viral DNA sequences of genes encoding the ATPase and the major capsid protein of tropical iridovirus isolates which are pathogenic to fishes in Japan, South China Sea and Southeast Asian countries. Arch Virol 147:2089–2109

Waltzek TB, Marty GD, Alfaro ME, Bennett WR and others (2012) Systemic iridovirus from threespine stickleback *Gasterosteus aculeatus* represents a new megalocytivirus species (family *Iridoviridae*). Dis Aquat Org 98:41–56

Waltzek TB, Miller DL, Gray MJ, Drecktrah B and others (2014) New disease records for hatchery-reared sturgeon. I. Expansion of frog virus 3 host range into *Scaphirhynchus albus.* Dis Aquat Org 111:219–227

Wang CS, Shih HH, Ku CC, Chen SN (2003) Studies on epizootic iridovirus infection among red sea bream, *Pagrus major* (Temminck & Schlegel), cultured in Taiwan. J Fish Dis 26:127–133

Wang CS, Chao SY, Ku CC, Wen CM, Shih HH (2009) PCR amplification and sequence analysis of the major capsid protein gene of megalocytiviruses isolated in Taiwan. J Fish Dis 32:543–550

Wang S, Huang X, Huang Y, Hao X and others (2014) Entry of a novel marine DNA virus, Singapore grouper iridovirus, into host cells occurs via clathrin-mediated endocytosis and macropinocytosis in a pH-dependent manner. J Virol 88:13047–13063

Wang YQ, Lu L, Weng SP, Huang JN, Chan SM, He JG (2007) Molecular epidemiology and phylogenetic analysis of a marine fish infectious spleen and kidney necrosis virus-like (ISKNV-like) virus. Arch Virol 152:763–773

Weber ES III, Waltzek TB, Young DA, Twitchell EL and others (2009) Systemic iridovirus infection in the Banggai cardinalfish (*Pterapogon kauderni* Koumans 1933). J Vet Diagn Invest 21:306–320

Wen CM, Hong JR (2016) Complete genome sequence of a giant sea perch iridovirus in Kaohsiung, Taiwan. Genome Announc 4:e01759-15

Yanong RP, Waltzek TB (2016) Megalocytivirus infections in fish, with emphasis on ornamental species (FA182). University of Florida Institute of Food and Agricultural Sciences, Gainesville. http://edis.ifas.ufl.edu/fa182 (accessed 24 Feb 2017)

Zhang BC, Zhang M, Sun BG, Fang Y, Xiao ZZ, Sun L (2013) Complete genome sequence and transcription profiles of the rock bream iridovirus RBIV-C1. Dis Aquat Org 104: 203–214

Editorial responsibility: James Jancovich, San Marcos, California, USA

Submitted: December 6, 2017; Accepted: May 20, 2018
Proofs received from author(s): August 6, 2018